

Radiation Physics and Chemistry

Observation of Self-Healing and Blue Response Enhancement in c-Si Solar Cells Exposed to Electron Irradiation

--Manuscript Draft--

Manuscript Number:	RPC-D-24-01859
Article Type:	Full Length Article
Keywords:	Solar cell; electron irradiation; Aged c-Si solar cell; Electrical characterization; Self-healing effect
Abstract:	The effects of electron irradiation on the performance of mono-crystalline silicon (c-Si) solar cells were investigated by examining various electron doses, ranging from 225 to 900 Gy, with an energy of 8 MeV. The study focused on dose-dependent degradation in cell behavior resulting from irradiation. Detailed analysis was conducted through dark and illuminated current-voltage (I-V) measurements, external quantum efficiency (EQE) measurements, capacitance-voltage (C-V) measurements, and conductance-voltage (G/ω-V) measurements. The observed degradations were thoroughly analyzed, quantified, and discussed by comparing the results obtained from complementary electrical and optical characterizations of the cells before and after irradiation. The experimental findings indicated that the degradation in cell parameters was attributed to irradiation-induced defect formations in the base layer. However, the devices were found to be resilient to defect formations in the emitter and near the depletion edge of the base. After 52 months of irradiation, significant self-healing effects and improvements in blue response were observed in the cells, likely due to additional positive charge formation in the nitride layer from oxynitride formation in the ambient atmosphere over time, accelerated by radiation damage. This was confirmed by both illuminated I-V and EQE measurements.

- We report effects of electron irradiation on c-Si solar cells with varying electron doses.
- Irradiation effects studied through electrical and spectral response measurements in a complementary way.
- The performance of aged c-Si solar cells was investigated again after 52 months later.
- Room temperature self-healing effect was observed after 52-month period of irradiation.
- Remarkable enhancement was observed in the blue response of the cells after 52-month period compared to the unirradiated and just irradiated cell responses.

Observation of Self-Healing and Blue Response Enhancement in c-Si Solar Cells Exposed to Electron Irradiation

Ismail Kabacelik^{1*} Mustafa Kulakci^{2,3}

¹ Department of Medical Services and Techniques, Vocational School of Health Services, Bartın University, 74100, Bartın, Turkey

² Department of Physics, Eskisehir Technical University, 26470 Eskişehir, Turkey

³ Institute of Earth and Space Sciences, Eskisehir Technical University, 26470, Eskişehir, Turkey

Abstract

The effects of electron irradiation on the performance of mono-crystalline silicon (c-Si) solar cells were investigated by examining various electron doses, ranging from 225 to 900 Gy, with an energy of 8 MeV. The study focused on dose-dependent degradation in cell behavior resulting from irradiation. Detailed analysis was conducted through dark and illuminated current-voltage (I-V) measurements, external quantum efficiency (EQE) measurements, capacitance-voltage (C-V) measurements, and conductance-voltage (G/ω -V) measurements. The observed degradations were thoroughly analyzed, quantified, and discussed by comparing the results obtained from complementary electrical and optical characterizations of the cells before and after irradiation. The experimental findings indicated that the degradation in cell parameters was attributed to irradiation-induced defect formations in the base layer. However, the devices were found to be resilient to defect formations in the emitter and near the depletion edge of the base. After 52 months of irradiation, significant self-healing effects and improvements in blue response were observed in the cells, likely due to additional positive charge formation in the nitride layer from oxynitride formation in the ambient atmosphere over time, accelerated by radiation damage. This was confirmed by both illuminated I-V and EQE measurements.

Keywords: Solar cell; Electron irradiation; Aged c-Si solar cell; Electrical characterization; Self-healing effect

* Corresponding author: Ismail Kabacelik
E-mail address: ikabacelik@gmail.com

1. Introduction

Photovoltaic (PV) has been a fast-growing market for the last decades to close the gap in increasing electrical energy demand in a sustainable way by using solar energy as being the largest among renewable energy sources. Today, the PV industry is overwhelmingly dominated by c-Si technology with a market share of over %90 in terrestrial applications (Yu et al., 2022). Although c-Si cell technology was the pioneer of the space utilization of PV and has kept its dominance in this area for a long time, its dominance has been superseded by group III-V semiconductor cell technology. Recently, Si has regained significant interest due to the widespread progress in space and aerospace technologies, which require large-scale and relatively cost-effective installations. Highly efficient new cell technologies based on hybrid integration of Si and III-V technologies either by mechanical or wafer bonding techniques have been pursued to provide a viable solution for flourishing market requirements in a reliable and cost-effective way (Cariou et al., 2018; Medjoubi et al., 2021; Mizuno et al., 2022). Besides its cost-effectiveness, Si is a good alternative to Ge as a bottom cell due to its superior properties much suitable for space environment, such as mechanical robustness, radiation and temperature tolerances (Essig et al., 2017; Medjoubi et al., 2021; Sharma et al., 2022; Yu et al., 2022).

Solar cells used in space applications are exposed to high-temperature cycles, wide range of charged and uncharged radiations that adversely affect cell performances (Hamache et al., 2016; Luft, 1964; Nikolić et al., 2015; Pellegrino et al., 2019; Sato et al., 2009; Yang et al., 2011). Therefore, cells to be used in that harsh environment inevitably require not only high-efficiency values with a high watt/kg ratio but also high tolerances to that hard condition for stable and long-term reliable use in space platforms. Today only a few material systems can provide all these requirements and prove themselves over long-term use in numerous different tasks. Besides group III-V materials and c-Si, recently Cu(In,Ga)Se₂ (CIGS) and perovskite-based materials have taken huge interest as an emerging alternative candidate owing to their attractive properties such as radiation hardness, cost-effectiveness and functionality over flexibility and lightweightness (Jasenek and Rau, 2001; Kawakita et al., 2002; Lang et al., 2016; Yang et al., 2020).

As the irradiation by high energy particles introduces defect formations in solar cells (Srour et al., 2003; Zhang et al., 2020), it is critical to understand the behavior of the cells that exposed to those radiations for the reliability and longevity of the utilization. Mainly two effects occur in the cell structure as a result of interaction with the energetic particles; the first one is ionization and the second one is displacement damage (Danilchenko et al., 2008; Summers et al., 1995; Zhang et al., 2014). The ionization effect is the generation of electron-hole pairs in

the base layer of the cell. The displacement damage is the movement of atoms from their initial position in the crystal lattice to another position where they are electrically inactive. These induced defects produce generally deep energy levels in the band gap of the cell material (Ali et al., 2016; Nikolić et al., 2013). Then those defects mostly act as traps and recombination centers that cause to degradation in lifetime and diffusion length of minority carriers in the base of the cell and could cause to increased resistivity due to a reduction in the majority carriers (Bhat et al., 2014; Yan et al., 2020; Zdravković et al., 2011). As a result of all effects, significant degradations could be observed in the output parameters of the cells (Hisamatsu et al., 1998; Shen et al., 2019; Tobnaghi et al., 2014; Weiss et al., 2020).

After successful demonstration on Vanguard I, Si cell had become the indispensable choice of cell technology for space applications for a long time (Essig et al., 2016; Green, 2016; Schnabel et al., 2020). To understand the effects of space conditions on Si cell performance, irradiation studies have been initiated as early as the 60s and keeping its importance up to date (Junga and Enslow, 1959; Luft, 1964). Those studies that mimicking the space environment have led to the development of more tolerant Si cells in terms of design and material (Schygulla et al., 2022; Verduci et al., 2022). Although degradation mechanisms in Si cells well understood with respect to different aspects of energetic particles like particle type, fluence, energy etc., there is a huge room about recovery after irradiation, especially on self-healing effects without applications of any external agents on the cells.

In this study, the effects of 8 MeV electron irradiation on the c-Si solar cell performance have been investigated extensively and in detail for different doses. Electrical and optoelectronic characterization techniques have been used to evaluate the electron-induced degradations in the device characteristics of the cells before and after irradiation. After 52 months of irradiation cell parameters were measured again at the same conditions that of before to reveal any possible effect of time. A remarkable self-healing effect has been observed in the cells kept at room temperature whose strength depends on electron dose and quantified through recovery in the cell parameters. The quantification of recovery in the cell parameters has been reached via comparative assessment of the successive measurement results of unirradiated and irradiated cells. Moreover, significant enhancement was observed in the blue response of the cells after 52 months of irradiation compared to that of unexposed ones, which could shed a light to understand and develop new insights for the passivation of Si solar cells.

1 **2. Materials and methods**

2 The solar cells were fabricated using Czochralski-grown (Cz) mono-crystalline, (100)
3 oriented, p-type Si wafer (boron-doped $\sim 5 \times 10^{16} \text{ cm}^{-3}$) with a resistivity of 1-3 Ωcm , with a
4 thickness of 160 μm , and with dimensions of 156 mm x 156 mm. The emitter layer (n) was
5 formed by phosphorus diffusion with a concentration of $5 \times 10^{20} \text{ cm}^{-3}$. Details of the cell
6 fabrication process are given elsewhere Ref (Es et al., 2016) and (Kulakci et al., 2013).
7
8
9

10 Following the device fabrication, the cell was cut into smaller pieces with an area of 2.8
11 cm^2 by using a laser. Then, the electrical characteristics and spectral responses of each cell were
12 measured before and after electron irradiation. Dark I-V measurements were performed by
13 Keithley 2440 source-meter. Illuminated I-V measurements were performed under AM1.5G
14 condition using Abet 2000 solar simulator. The spectral response of the cells was measured in
15 a wavelength range of 300 - 1100 nm and with an interval of 10 nm using Newport QuantX-
16 300 quantum efficiency measurement system. The C-V and G/ ω -V characteristics were carried
17 out under dark condition at a frequency of 100 kHz by using HP 4192A LF impedance analyzer.
18
19
20
21
22
23
24

25 Solar cells were exposed to electrons with an energy of 8 MeV and with a fluence of
26 $16 \times 10^{10} \text{ cm}^{-2}$ using a modified clinical linear accelerator (cLINAC, Philips SLI-25 LINAC).
27 Detailed information on cLINAC can be found at Ref (Boztosun et al., 2015). Four solar cells
28 were chosen and separately irradiated with different electron doses of 225, 450, 675 and 900
29 Gy respectively.
30
31
32
33

34 In this study, electrical and optical properties of c-Si solar cells were systematically
35 studied by means of dark and illuminated I-V, EQE, C-V and G/ ω -V measurements before and
36 after 8 MeV electron irradiation at various applied doses. After irradiation solar cells were kept
37 at ambient conditions at room temperature for 52 months and were characterized again to see
38 possible recovery/degradation in time.
39
40
41
42

43 **45 3. Results and discussions**

44 Room temperature dark I-V measurement results of solar cells before, just after and after
45 52 months of irradiation for different electron doses are shown comparatively in Fig. 1 and
46 diode ideality factors calculated by using single diode model from these curves are given in
47 Table 1. As seen in the table, with the increase in radiation dose, diode ideality factor goes to
48 increase which indication of creation of generation-recombination levels within the bandgap of
49 Si. After 52 months of irradiation, ideality factors close towards the unirradiated values which
50 indicates the annihilation of some of those levels in 52 months period of keeping the cells at
51 room temperature. The effect of electron irradiation is also clearly seen in the reverse bias
52
53
54
55
56
57
58
59
60
61
62
63
64
65

regime (Fig. 1), generation current increases in accordance with the dose level which is also consistent with the increase in ideality factor towards 2 (and over) in the forward bias regime because of increased recombination current with the act of these defects. As in the case of forward bias, the self-annihilation effect has been also seen in reverse bias after 52 months, excess generation currents reduced to the level of unirradiated devices.

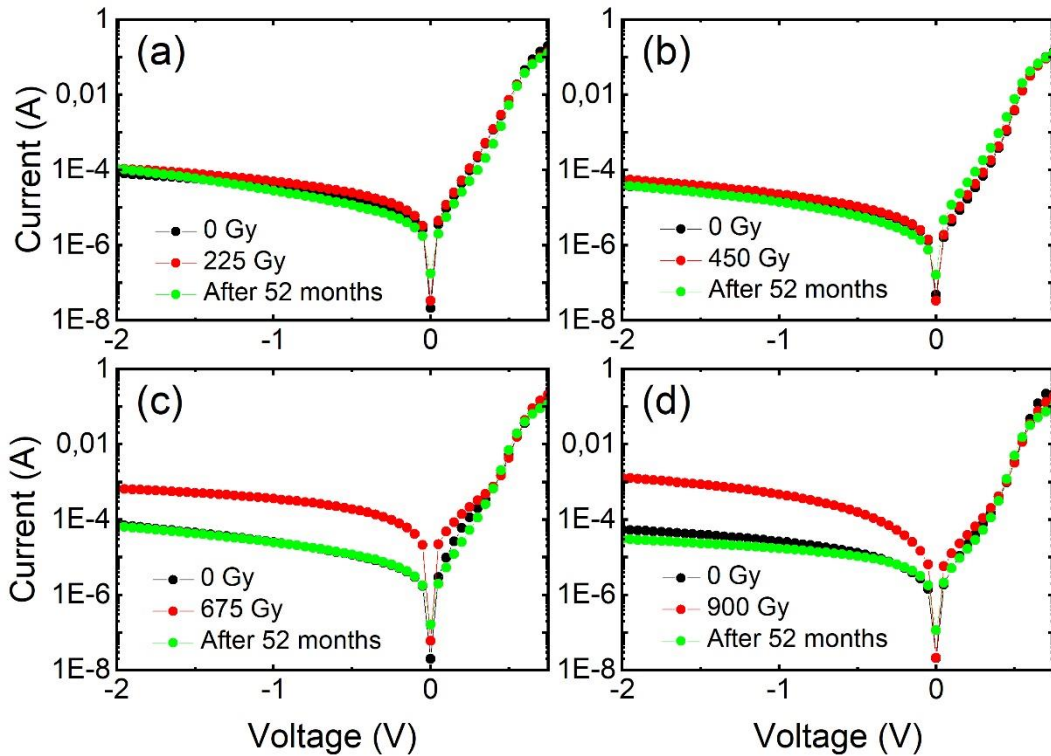


Figure 1. Room temperature dark I-V characteristics of the cells before, just after and after 52 months of irradiation for different electron doses.

Table 1. Calculated diode ideality factors of the cells.

	225 Gy	450 Gy	675 Gy	900 Gy
Unirradiated	1.71	1.67	1.62	1.76
Just after Irradiation	1.86	1.94	2.18	2.43
After 52 months of irradiation	1.74	2.08	1.95	2.13

The illuminated I-V characteristics of solar cells under AM1.5G condition before and after irradiation with different electron doses are shown in Fig. 2. As clearly seen, there is a reduction in both J_{sc} and V_{oc} values of cells after irradiation where the level of reductions follow an increase in electron dose. The decrease in J_{sc} and V_{oc} is due to the electron-induced

1 defects that act as recombination centers for the light-generated carriers before diffusing to the
 2 depletion region. As the density of defects increases with the radiation dose, carrier loss
 3 becomes more pronounced in a monotonous way (Giesecke et al., 2011; Horiuchi et al., 2000),
 4 even for aggressively higher dose levels anomalous degradation in cell outputs could be
 5 observed (Morita et al., 1997). When considering the energy of the impacting electrons, the
 6 origin of those defects assumed to be displaced Si atoms from their lattice sites (Bhat et al.,
 7 2015), and manifest themselves on the carrier's lifetime/diffusion length, especially in the base
 8 layer of the cells (Ashry and Fares, 2003; Bhat et al., 2014; Kuendig et al., 2003; Taylor et al.,
 9 1997). After irradiation, cells were kept at ambient conditions at room temperature for 52
 10 months to see any recovery/degradation in time. When looking at the comparative I-V curves
 11 in the figure, one can easily see varying self-recovery behavior in the cell parameters depending
 12 on radiation dose, which is much remarkable in the J_{SC} . The degree of improvement is the
 13 greatest in the cell irradiated with the lowest dose of electron and is monotonously decreasing
 14 with the increase in dose level. Observed room temperature self-healing effects in the J_{SC}
 15 discussed in detail below together with EQE results. Small improvement was also observed in
 16 V_{OC} values, but it is not substantial as in the case of J_{SC} .
 17
 18
 19
 20
 21
 22
 23
 24
 25
 26
 27
 28
 29
 30
 31
 32
 33
 34
 35
 36
 37
 38
 39
 40
 41
 42
 43
 44
 45
 46
 47
 48
 49
 50
 51
 52
 53
 54
 55
 56
 57
 58
 59
 60
 61
 62
 63
 64
 65

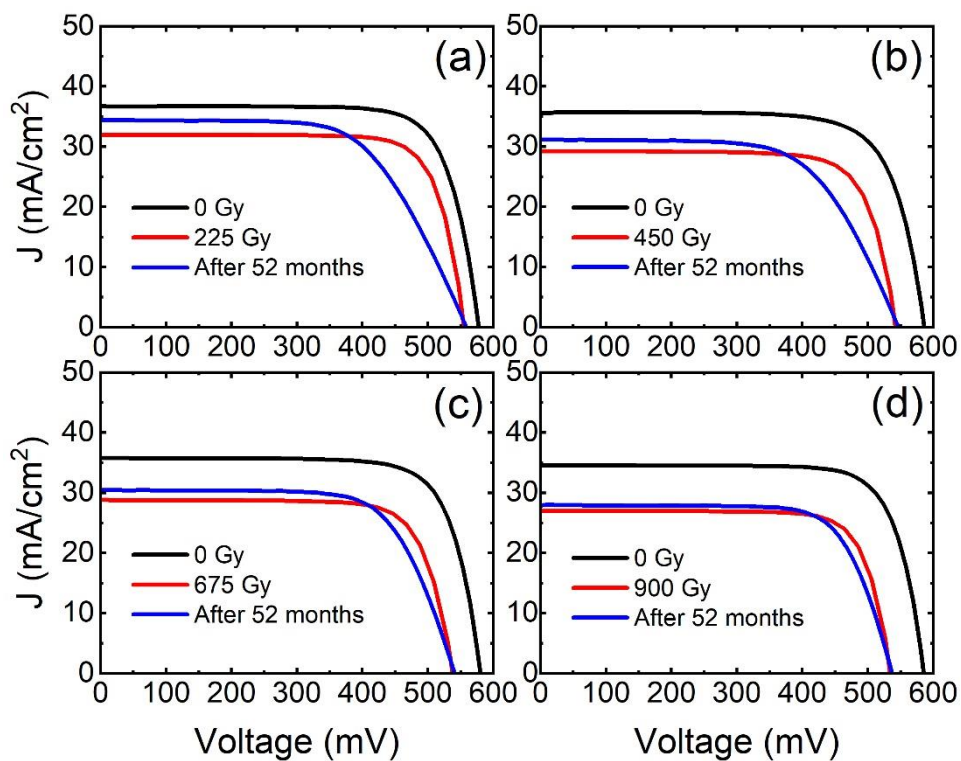


Figure 2. Illuminated J-V curves of c-Si solar cells before and just after irradiation with different electron doses. J-V curve of cells after 52 months of irradiation is also given to see recovery effect.

Fig. 3(a) shows the normalized parameters of just-irradiated cells such as FF, V_{oc} , J_{sc} and η determined from the illuminated J-V characteristics for different electron doses. All cell parameters were normalized separately by the parameters obtained before irradiation to see the effects of radiation dose clearly. Contrary to other parameters of the cells no degradation has been observed in the FFs after irradiation, indeed slight enhancements are clearly seen. As seen in the figure, there is a significant loss in conversion efficiencies depending on the dose level. The loss in efficiency increases from %15 to %28 with the radiation dose of 225 Gy (lowest dose) and 900 Gy (highest dose) respectively. However, in a noticeable way, the rate of efficiency loss goes to decrease with an increase in dose level. The loss in J_{sc} is %13 at the lowest dose and reaches to %22 in the cell irradiated with the highest dose, the observed V_{oc} losses for these limiting dose values are %4 and %8 respectively. Irrespective of the dose levels, the losses in conversion efficiencies are mainly determined by the degradation in J_{sc} compared to contribution from V_{oc} . The degradation in cell parameters, especially in J_{sc} has been elaborated deeply with the conjunction of EQE measurement results.

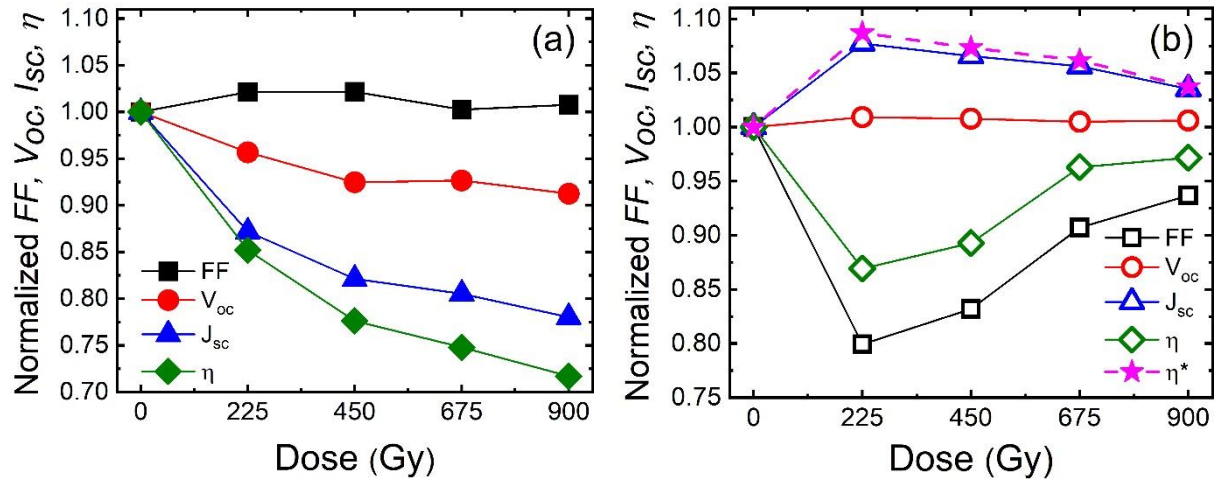


Figure 3. Normalized cell parameters of the cells with different dose values: (a)Normalized parameters of the cells with respect to their unirradiated values, (b) Normalized cells parameters obtained after 52 months of irradiation with respect to their just irradiated values. Starred efficiency (η^*) represents the projected normalized efficiencies of the cells after 52 months of irradiation with respect to their just irradiated values by keeping the normalized FFs as being unity.

Fig. 3(b) shows the parameters of the cells measured after 52 months of irradiation which are normalized by the parameters obtained by measurements just after irradiation. Room temperature self-healing has been observed in the cells without applying any external agent like heat treatment etc., the cells were only preserved in ambient conditions for 52 months. Small

enhancement has been observed in V_{OC} for all dose values. As clearly seen, the observed recovery in J_{SC} values is remarkable which means that significant part of the defects generated by radiation has been cured somehow over the 52 months period. The recovered part of J_{SC} is maximum for the lowest dose irradiation and monotonously decreases with an increase in dose level. The calculated recovered percentage in J_{SC} values due to self-healing effects is given in Table 2. The percentage of recovery in J_{SC} is 16.2 % for the highest irradiation dose and reaches as high as 52.6 % for the lowest dose. More details on the recovery in current will be given in the EQE part. Although one expects enhancement in the conversion efficiencies regarding the recovery in corresponding voltage and current values, efficiency results do not reflect the expectations as seen in Fig. 3(b). The reduction in efficiencies (compared to just irradiated values) solely depends on the degradation in FFs. As clearly seen in the figure, the efficiency-dose curve directly follows the behavior of FF-dose curve with almost the same functional dependence with respect to dose level. The main reason in FF degradation after 52 months of irradiation was found to be a drastic increase in the series resistance of the cells (Fig. 4). The shunt resistances had insignificant changes after 52 months compared to ones obtained from the measurements just done after irradiation of the cells (not shown here). For the case just after irradiation, series resistance increases with an increase in dose level. A drastic increase in series resistances has been observed after 52 months compared to just irradiated ones. Contrary to just-irradiated cells behavior, the series resistance decreases in a monotonous way with an increase in radiation dose (See Fig. 4). Although there has been a significant recovery in J_{SC} values over a 52-month period, the expected improvement in conversion efficiencies has been seriously hindered by the degradation in FFs caused by the drastic increase in series resistances. Assuming that there has been no further degradation in FF of the irradiated cells during this period, the projected conversion efficiencies were calculated and are presented in Fig. 3(b) as a dashed curve. According to this projection, a total of 8.7% and 3.7% of efficiency loss were recovered caused by irradiation for the lowest and highest doses, respectively. It is noteworthy that the recovery in short circuit current is primarily responsible for the improvement in efficiency, as can be observed from the comparison of the current-dose and efficiency-dose curves in Fig. 3(b) with respect to irradiation levels.

Table 2. Calculated loss and recovery in J_{SC} values from illuminated I-V measurements (Fig. 2) for different radiation doses. J_{SC0} , J_{SC1} and J_{SC2} are the short circuit current densities of the cells before irradiation, just after irradiation and after a 52-month period of irradiation respectively.

Dose (Gy)	Loss in J_{SC} ($J_{SC0} - J_{SC1}$) (mA/cm ²)	Recovery in J_{SC} ($J_{SC2} - J_{SC1}$) (mA/cm ²)	Percentage in J_{SC} recovery (%)
225	4.70	2.47	52.6
450	6.37	1.92	30.1
675	6.97	1.62	23.2
900	7.60	1.23	16.2

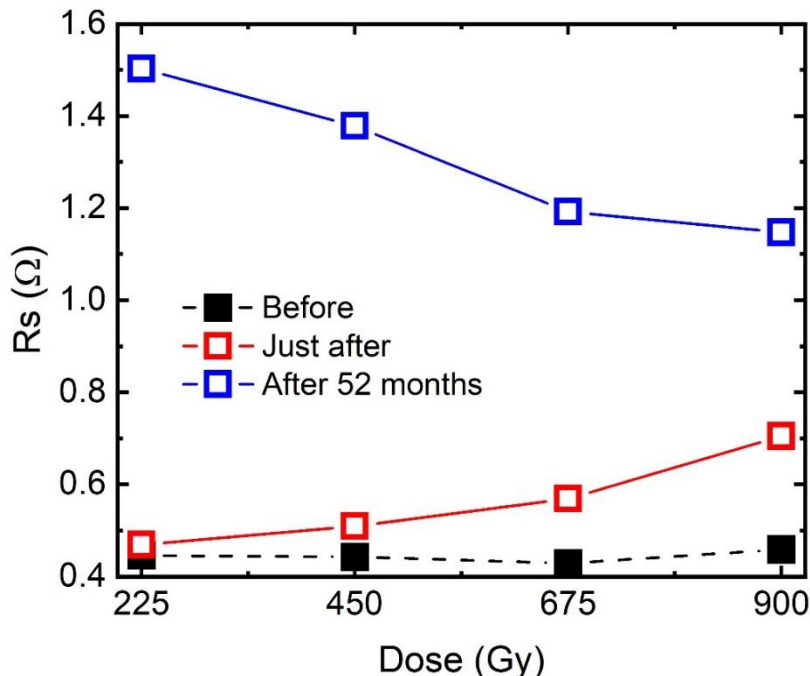


Figure 4. Effects of irradiation on the series resistance obtained from illuminated I-V measurements.

EQE measurement is a valuable method to understand the behavior of the cell with respect to specific region of incoming photon wavelength. To thoroughly investigate the degradation effects of electron irradiation on the cells and to determine the potential mechanisms responsible for the self-healing effects observed in the recovery of short circuit current, EQE measurements were conducted. The findings of these measurements are presented comparatively in Fig. 5. Based on the results shown in Fig. 5, a significant decrease in EQE values can be observed in the long-wavelength region of the spectrum, and this loss in the red

response becomes more prominent with increasing levels of irradiation. It is noteworthy that electron irradiation did not cause any changes in the reflectivity properties of the cells, and no observable changes were detected in the EQE results of an unirradiated cell measured at the beginning of the study and after 52 months (Fig. 6). Instead, the reduction in EQE is directly attributed to the decline in carrier collection due to generated defects in the active regions of the devices, as illustrated in Fig. 6. On the other hand, EQE results suggest that solar cells have high tolerance to defects in the blue response region of the spectrum as the light absorbed close to the surface. Upon examination of Fig. 5, a distinct demarcation can be observed on the high-energy side of the curves. Beyond this point, towards the lower wavelength region of the spectrum, no detrimental effects on the cell response were observed. In fact, a very slight improvement can be seen in the curves. For the lowest dose (225 Gy), the border onset is approximately at a wavelength of 654 nm, while for higher doses, this onset systematically shifts towards lower wavelengths and reaches around 535 nm for the highest irradiation dose (900 Gy). Considering the absorption depth of these wavelengths of light in Si, the onset points, at which the loss of minority carrier collection begins, are situated at approximately 3.5 μ m from the surface of the cells for the lowest dose, and this depth decreases to around 1.1 μ m for the highest dose. The cells have an emitter depth of 500 nm, and the depletion layer width in the absorber region is calculated to be around 300 nm. This indicates that for the highest irradiation dose, recombination loss begins in the immediate vicinity of the depletion region, and as the dose decreases, the loss moves deeper into the absorber. Based on the behavior of the curves, it can be inferred that there is no carrier loss observed in the emitter and depletion layers, even when subjected to the highest dose of electron irradiation, as compared to the response of unirradiated cells. The EQE results suggest that the degradation observed in the solar cells after electron irradiation can be attributed to the formation of defects in the base layer (Bhat et al., 2014; Yamaguchi, 2001). These defects cause a reduction in the minority carrier diffusion length or minority carrier lifetime, resulting in carrier collection loss due to recombination (Babaei and Ghozati, 2017). In the EQE results, the decrease in efficiency for longer wavelength photons in the spectrum is mainly attributed to absorption deeper in the absorber layer and towards the back contact, which results in significant loss of carrier collection, and this loss behavior is found to depend on the irradiation dose. The observed carrier loss behavior in EQE is well-correlated with the dose dependence of J_{SC} values obtained from the illuminated I-V curve of the cells just after irradiation (see Fig. 2, Fig. 3, and Table 2).

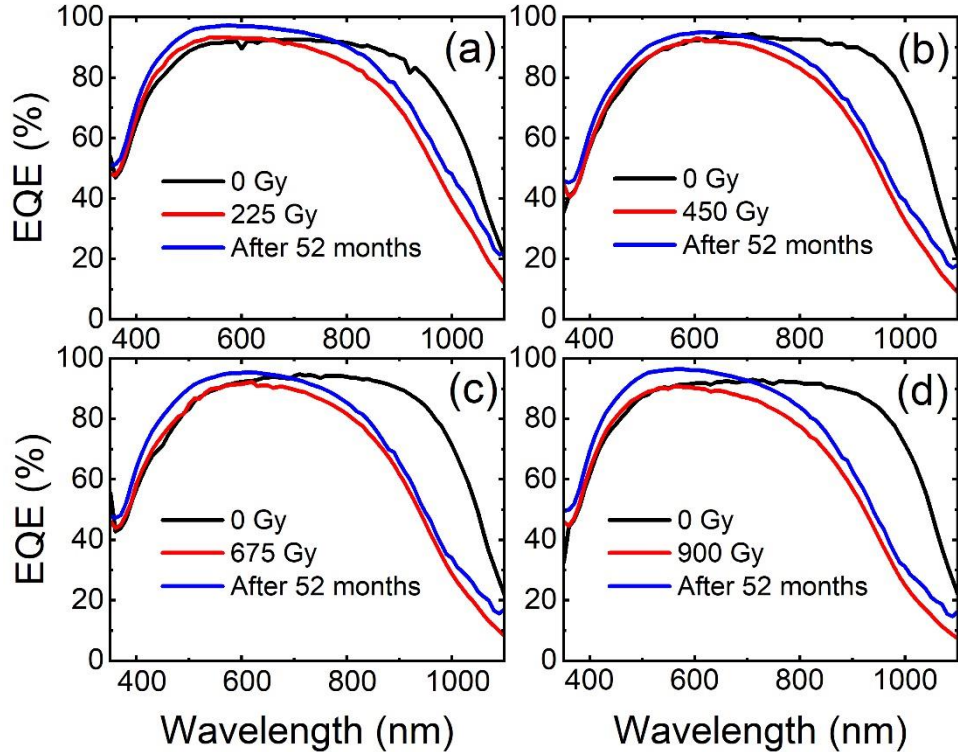


Figure 5. The EQE spectrum of the cells measured before and just after and after 52 months of irradiation.

Fig. 5 also shows the EQE measurement results of the cells after 52 months of irradiation. There is an enhancement in the EQE response for all dose values across the entire spectrum compared to the results obtained immediately after irradiation. A significant increase in the blue response of the cells is observed in the curves, which is even higher than the blue response of the unirradiated cells. This enhancement in blue response could be due to the formation of positive charges in the silicon nitride layer over time, which might cause field effect passivation on the emitter surface by pushing minority carriers (holes) away from the interface. It is well known that excess positive charges related with K (+) center in silicon nitride serve as an effective field-effect passivation in silicon solar cells especially on n-type emitter (Leguijt et al., 1996; Lelièvre et al., 2009; Sharma et al., 2013). At room temperature, ambient oxidation could form oxynitride formation in silicon nitride film which enhances extra positive charge formation over oxygen-correlated bond defects in time which may boost field effect passivation over 52 months period (Raider et al., n.d.; Schmidt and Aberle, 1999). Most probably due to radiation-induced damages this charge formation could be boosted and result in good surface passivation which is not observed in unirradiated cell (Robertson, 1993). Upon examining Fig. 5, it can be observed that the onset of carrier loss shifts to higher wavelengths compared to the results immediately after irradiation, with the switch occurring from around

654 nm to 786 nm for the lowest dose and from about 535 nm to 700 nm for the highest dose.
 In terms of the absorption depth of these wavelengths, the onset of carrier loss shifts from 3.5
 μm to 9.6 μm for the lowest dose and from 1.1 μm to 5.0 μm for the highest dose, respectively.
 For doses in between, the recovery in EQE response is slightly lower compared to these
 extremes. The EQE curves suggest that the improvements in carrier collection could be
 attributed to the reordering of radiation-induced defects over time at room temperature, which
 could be referred to as the room temperature annealing or self-healing effect. The enhancement
 and partial recovery in EQE over 52 months (Fig. 5) are consistent with the recovery in short-
 circuit current behavior (Fig. 2 and Fig. 3) obtained from illuminated I-V measurements.

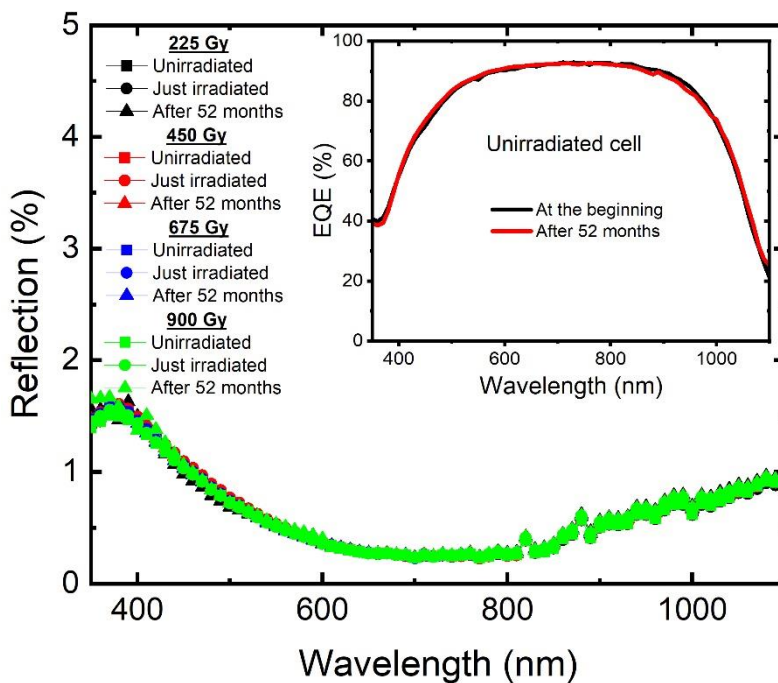


Figure 6. Reflectivity measurement results of the cells before, just after and after 52 months of irradiation. The inset shows the EQE spectrum of the unirradiated sample at the beginning and after 52 months.

As the EQE is the spectral distribution of photocurrent, short circuit current values of the cells also calculated using Eq.1.

$$J_{sc} = \int EQE(\lambda) J_{\gamma, AM1.5G}(\lambda) d\lambda \quad (1)$$

where, $J_{\gamma, AM1.5G}(\lambda)$ is the incident photon current density per wavelength interval, derived from AM1.5G data taken from ASTM G173-03 reference spectrum.

To determine the loss and the self-healing effects in currents, the J_{sc} values calculated from EQE curves of cells for the cases of unirradiated, just irradiated, and after 52 months of

irradiation are compared in Table 3, in a similar way as done in the illuminated I-V
 1 measurements. As seen from the table, the irradiation loss in current increases monotonously
 2 with an increase in dose level which is consistent with results that were obtained from the solar
 3 simulator measurements (Table 2). However, the degree of current losses measured under a
 4 solar simulator is slightly higher than ones calculated from EQE measurements. Based on the
 5 calculations using EQE spectrum, in a 52-month period after irradiation, 81.5% of the loss in
 6 current recovered back for the device subject to the lowest electron dose and it is about 44.3%
 7 for the highest dose respectively. For the dose levels in between them, the calculated recovery
 8 in current is relatively low compared to these extremes. The recovery in short circuit currents
 9 calculated from EQE measurements is higher than that obtained from solar simulator
 10 measurements (Table 3 and Table 2). The differences observed loss in current levels just after
 11 irradiation and recovery in currents due to self-curing effects between the solar simulator and
 12 EQE measurement might be results of difference in illumination area on the cells. In solar
 13 simulator measurements the whole area of the cells was illuminated, on the other hand in EQE
 14 measurements the illumination area was only 2 mm². The cells used here are laser cut from a
 15 243 cm² cell into a small size of 2.8 cm². The laser cut processing unavoidably damages the
 16 edges of the cells, which introduces extra recombination and leak pathways, and this could
 17 lower the current in solar simulator measurement due to extra carrier losses over the defective
 18 edges.
 19
 20
 21
 22
 23
 24
 25
 26
 27
 28
 29
 30
 31
 32
 33
 34
 35

Table 3. Calculated loss and recovery in J_{SC} values from EQE measurements (Fig. 5) for different radiation doses. J_{SC0}, J_{SC1} and J_{SC2} are the short circuit current densities of the cells for unirradiated, just irradiated and after 52 months of irradiation cases respectively.

Dose (Gy)	Loss in J _{SC} (J _{SC0} – J _{SC1}) (mA/cm ²)	Recovery in J _{SC} (J _{SC2} – J _{SC1}) (mA/cm ²)	Percentage in J _{SC} recovery (%)
225	2.75	2.24	81.5
450	4.62	1.73	37.4
675	5.36	1.89	35.3
900	5.87	2.60	44.3

Fig. 7 and 8 show the C-V and G/ ω -V results of the cells measured at room temperature under dark conditions, with an AC signal of 100 kHz. For all unirradiated cells, the capacitance increases from reverse biases (geometric capacitance) towards forward bias as the depletion width decreases, with a negligible change in conductance. With the onset of bias voltage where conductance rapidly increases, the capacitance of the cells rapidly increases due to the storage (diffusion) capacitance of minority carrier injection up to a peak value. Then in the very high injection regime, the capacitance decreases as well as a slight decrease in conductance. After electron irradiation, almost any change observed in the capacitance and conductance values in the reverse bias case. However, in the forward bias regime, both conductance and capacitance have lower values compared to the unirradiated case. It is supposed to decrease in the minority carrier injection efficiency due to recombination through defects created by radiation causes both a decrease in diffusion capacitance and conductance. No significant changes were observed in the capacitance and conductance behavior of the cells after irradiation for 52 months.

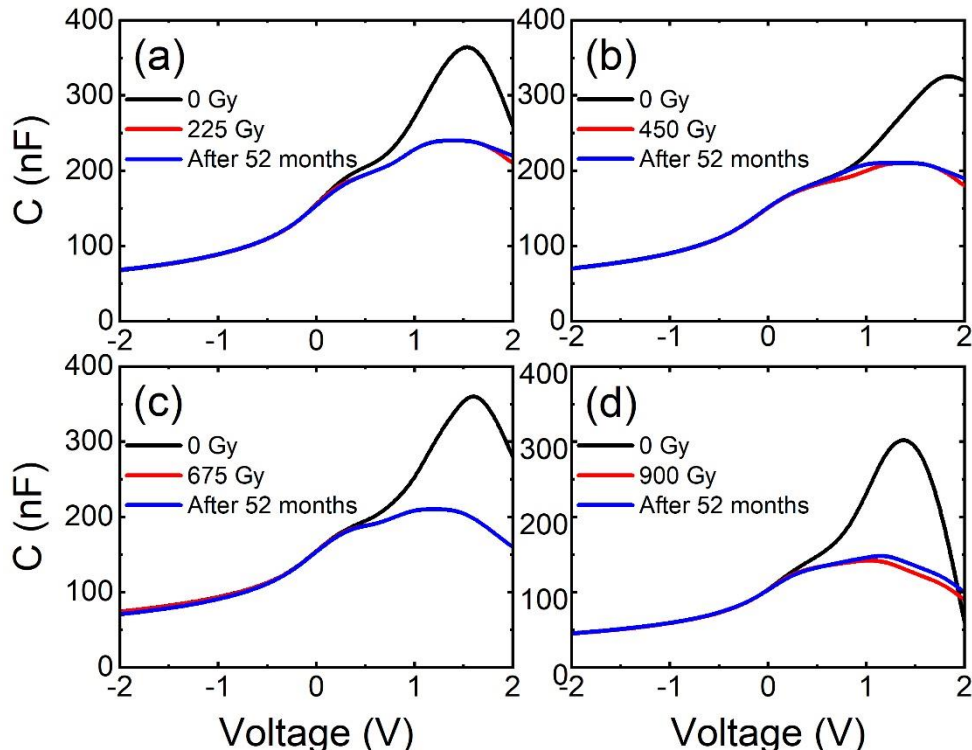


Figure 7. Capacitance-voltage characteristics of cells before, just after and after 52 months of irradiation taken under dark conditions for different electron doses.

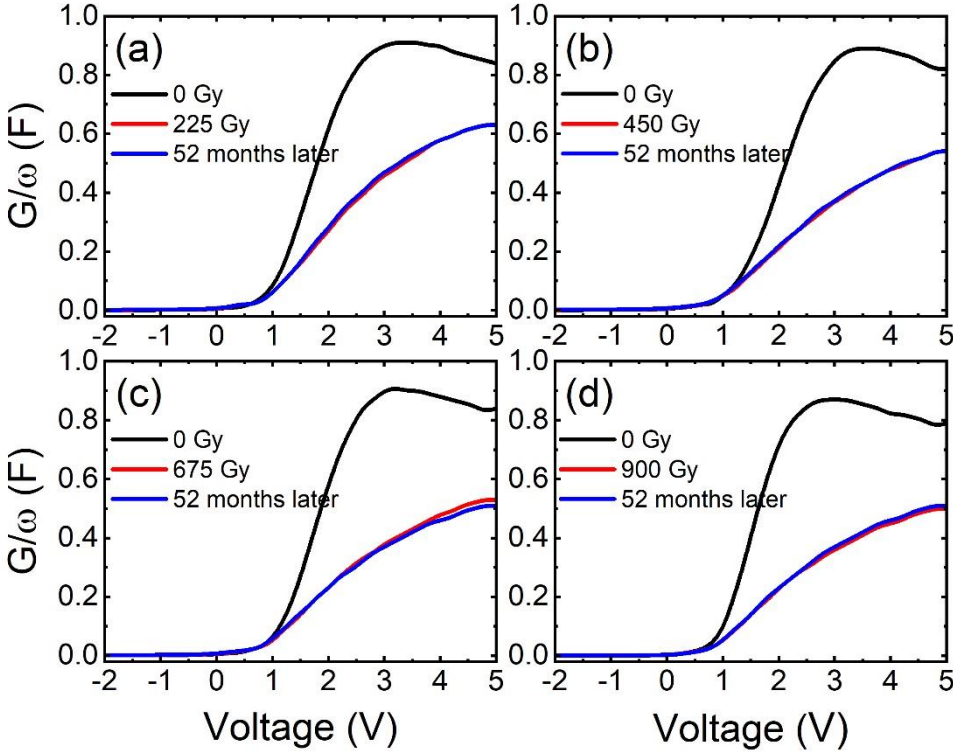


Figure 8. Conductance-voltage characteristics of cells before, just after and after 52 months of irradiation, taken under dark conditions for different electron doses.

4. Conclusions

This study investigated the effects of 8 MeV electron irradiation at different dose levels on c-Si solar cells and their recovery at room temperature after 52 months of irradiation. The experimental results, which compared the different doses, showed a degradation in cell parameters due to radiation-induced defects. As the electron dose level increased from the lowest to the highest dose, there was a significant reduction in efficiency values, with an efficiency loss increasing from 15% to 28%. The primary contribution to the loss of efficiency was due to a reduction in J_{SC} values, compared to moderate loss in V_{OC} . After 52 months of irradiation, a self-healing effect was observed in the devices, particularly as a remarkable recovery in the J_{SC} values. The recovery in current values was consistently verified by illuminated I-V and EQE measurements. Additionally, after 52 months of irradiation, a significant enhancement in the blue response of the cells was observed compared to the unirradiated cells, which was verified by EQE measurements. This enhancement assumed to be due to extra positive charge formation in silicon nitride film as a result oxynitrate formation in ambient atmosphere in time which could be boosted by defects formed by radiation. The observed enhancement in the blue response could pave the way for new passivation approaches for Si solar cells.

1
2
3
4
5
6
7
8
Acknowledgements

9
The author acknowledges the Center for Solar Energy Research and Applications (ODTÜ-GÜNAM) for sample preparation and characterization and the Akdeniz University Nuclear
10
Science Research and Application Center for irradiation facility.
11
12
13
14

15
16
References
17
18
19

- 20 Ali, K., Khan, S.A., MatJafri, M.Z., 2016. Improved radiation resistant properties of electron
21 irradiated c-Si solar cells. *Radiation Physics and Chemistry* 125, 220–226.
22 https://doi.org/10.1016/j.radphyschem.2016.04.015
23
Ashry, M., Fares, S., 2003. Diffusion length analysis and measurement in the base region of
24 photodiodes. *Journal of Physics and Chemistry of Solids* 64, 2429–2431.
25 https://doi.org/10.1016/S0022-3697(03)00285-3
26
Babaee, S., Ghozati, S.B., 2017. The study of 1 MeV electron irradiation induced defects in
27 N-type and P-type monocrystalline silicon. *Radiation Physics and Chemistry* 141, 98–
28 102. https://doi.org/10.1016/j.radphyschem.2017.06.012
29
Bhat, P.S., Rao, A., Krishnan, S., Sanjeev, G., Puthanveettil, S.E., 2014. A study on the
30 variation of c-Si solar cell parameters under 8 MeV electron irradiation. *Solar Energy
Materials and Solar Cells* 120, 191–196. https://doi.org/10.1016/j.solmat.2013.08.043
31
Bhat, P.S., Rao, A., Sanjeev, G., Usha, G., Priya, G.K., Sankaran, M., Puthanveettil, S.E.,
32 2015. Capacitance and conductance studies on silicon solar cells subjected to 8MeV
33 electron irradiations. *Radiation Physics and Chemistry* 111, 28–35.
34 https://doi.org/10.1016/j.radphyschem.2015.02.010
35
Boztosun, I., Đapo, H., Karakoç, M., Özmen, S.F., Çeçen, Y., Çoban, A., Caner, T., Bayram,
36 E., Saito, T.R., Akdoğan, T., Bozkurt, V., Kuçuk, Y., Kaya, D., Harakeh, M.N., 2015.
37 Photonuclear reactions with zinc: A case for clinical linacs. *Eur Phys J Plus* 130, 185.
38 https://doi.org/10.1140/epjp/i2015-15185-2
39
40 Cariou, R., Benick, J., Feldmann, F., Höhn, O., Hauser, H., Beutel, P., Razek, N.,
41 Wimplinger, M., Bläsi, B., Lackner, D., Hermle, M., Siefer, G., Glunz, S.W., Bett, A.W.,
42 Dimroth, F., 2018. III-V-on-silicon solar cells reaching 33% photoconversion efficiency
43 in two-terminal configuration. *Nat Energy* 3, 326–333. https://doi.org/10.1038/s41560-
44 018-0125-0
45
46 Danilchenko, B., Budnyk, A., Shpinar, L., Poplavskyy, D., Zelensky, S.E., Barnham, K.W.J.,
47 Ekins-Daukes, N.J., 2008. 1 MeV electron irradiation influence on GaAs solar cell
48 performance. *Solar Energy Materials and Solar Cells* 92, 1336–1340.
49 https://doi.org/10.1016/j.solmat.2008.05.006
50
51 Es, F., Kulakci, M., Turan, R., 2016. An Alternative Metal-Assisted Etching Route for
52 Texturing Silicon Wafers for Solar Cell Applications. *IEEE J Photovolt* 6, 440–446.
53 https://doi.org/10.1109/JPHOTOV.2016.2520207
54
55
56
57
58
59
60
61
62
63
64
65

- 1 Essig, S., Alleb  , C., Remo, T., Geisz, J.F., Steiner, M.A., Horowitz, K., Barraud, L., Ward,
2 J.S., Schnabel, M., Descoedres, A., Young, D.L., Woodhouse, M., Despeisse, M.,
3 Ballif, C., Tamboli, A., 2017. Raising the one-sun conversion efficiency of III-V/Si solar
4 cells to 32.8% for two junctions and 35.9% for three junctions. Nat Energy 2, 17144.
5 https://doi.org/10.1038/nenergy.2017.144
6
- 7 Essig, S., Steiner, M.A., Alleb  , C., Geisz, J.F., Paviet-Salomon, B., Ward, S., Descoedres,
8 A., LaSalvia, V., Barraud, L., Badel, N., Faes, A., Levrat, J., Despeisse, M., Ballif, C.,
9 Stradins, P., Young, D.L., 2016. Realization of GaInP/Si Dual-Junction Solar Cells with
10 29.8% 1-Sun Efficiency. IEEE J Photovolt 6, 1012–1019.
11 https://doi.org/10.1109/JPHOTOV.2016.2549746
12
- 13 Giesecke, J.A., Michl, B., Schindler, F., Schubert, M.C., Warta, W., 2011. Minority carrier
14 lifetime of silicon solar cells from quasi-steady-state photoluminescence. Solar Energy
15 Materials and Solar Cells 95, 1979–1982. https://doi.org/10.1016/j.solmat.2011.02.023
16
- 17 Green, M.A., 2016. Commercial progress and challenges for photovoltaics. Nat Energy.
18 https://doi.org/10.1038/nenergy.2015.15
19
- 20 Hamache, A., Sengouga, N., Meftah, A., Henini, M., 2016. Modeling the effect of 1 MeV
21 electron irradiation on the performance of n+-p-p+silicon space solar cells. Radiation
22 Physics and Chemistry 123, 103–108.
23 https://doi.org/10.1016/j.radphyschem.2016.02.025
24
- 25 Hisamatsu, T., Kawasaki, O., Matsuda, S., Nakao, T., Wakow, Y., 1998. Radiation
26 degradation of large fluence irradiated space silicon solar cells. Solar Energy Materials
27 and Solar Cells 50, 331–338. https://doi.org/10.1016/S0927-0248(97)00163-3
28
- 29 Horiuchi, N., Nozaki, T., Chiba, A., 2000. Improvement in electrical performance of
30 radiation-damaged silicon solar cells by annealing. Nucl Instrum Methods Phys Res A
31 443, 186–193. https://doi.org/10.1016/S0168-9002(99)01013-X
32
- 33 Jasenek, A., Rau, U., 2001. Defect generation in Cu(In,Ga)Se₂ heterojunction solar cells by
34 high-energy electron and proton irradiation. J Appl Phys 90, 650–658.
35 https://doi.org/10.1063/1.1379348
36
- 37 Junga, F.A., Enslow, G.M., 1959. Radiation Effects in Silicon Solar Cells. IRE Transactions
38 on Nuclear Science 6, 49–53. https://doi.org/10.1109/TNS2.1959.4315679
39
- 40 Kawakita, S., Imaizumi, M., Yamaguchi, M., Kushiyama, K., Ohshima, T., Itoh, H., Matsuda, S.,
41 2002. Annealing enhancement effect by light illumination on proton irradiated
42 Cu(In,Ga)Se₂ thin-film solar cells. Jpn J Appl Phys 41, L797–L799.
43 https://doi.org/10.1143/jjap.41.l797
44
- 45 Kuendig, J., Goetz, M., Shah, A., Gerlach, L., Fernandez, E., 2003. Thin film silicon solar
46 cells for space applications: Study of proton irradiation and thermal annealing effects on
47 the characteristics of solar cells and individual layers. Solar Energy Materials and Solar
48 Cells 79, 425–438. https://doi.org/10.1016/S0927-0248(02)00486-5
49
- 50 Kulakci, M., Es, F., Ozdemir, B., Unalan, H.E., Turan, R., 2013. Application of si nanowires
51 fabricated by metal-assisted etching to crystalline si solar cells. IEEE J Photovolt 3, 548–
52 553. https://doi.org/10.1109/JPHOTOV.2012.2228300
53
- 54
- 55
- 56
- 57
- 58
- 59
- 60
- 61
- 62
- 63
- 64
- 65

- Lang, F., Nickel, N.H., Bundesmann, J., Seidel, S., Denker, A., Albrecht, S., Brus, V. V., Rappich, J., Rech, B., Landi, G., Neitzert, H.C., 2016. Radiation Hardness and Self-Healing of Perovskite Solar Cells. *Advanced Materials* 28, 8726–8731. <https://doi.org/10.1002/adma.201603326>
- Leguijt, C., Lislegen, P., Eikelboom, J.A., Weeber, A.W., Schuurmans, F.M., Sinke, W.C., Alkemade, P.F.A., Sarro, P.M., Marte, C.H.M., Verhoef, L.A., 1996. Low temperature surface passivation for silicon solar cells, / *Solar Energy Materials and Solar Cells*.
- Lelièvre, J.-F, Fourmond, E., Kaminski, A., Palais, Olivier, Ballutaud, D., Lemiti, M., Lelièvre, J-F, Palais, O, 2009. Study of the composition of hydrogenated silicon nitride SiNx:H for efficient surface and bulk passivation of silicon. *Solar Energy Materials and Solar Cells* 93. <https://doi.org/10.1016/j.solmat.2009.01.023>
- Luft, W., 1964. Effects of Electron Irradiation on N on P Silicon Solar Cells. *IEEE Transactions on Aerospace* 2, 747–758. <https://doi.org/10.1109/TA.1964.4319662>
- Medjoubi, K., Lefèvre, J., Vauche, L., Veinberg-Vidal, E., Jany, C., Rostaing, C., Amalbert, V., Chabuel, F., Boizot, B., Cariou, R., 2021. Electrons irradiation of III-V//Si solar cells for NIRT conditions. *Solar Energy Materials and Solar Cells* 223, 110975. <https://doi.org/10.1016/j.solmat.2021.110975>
- Mizuno, H., Makita, K., Sai, H., Mochizuki, T., Matsui, T., Takato, H., Müller, R., Lackner, D., Dimroth, F., Sugaya, T., 2022. Integration of Si Heterojunction Solar Cells with III-V Solar Cells by the Pd Nanoparticle Array-Mediated “Smart Stack” Approach. *ACS Appl Mater Interfaces* 14, 11322–11329. <https://doi.org/10.1021/acsami.1c22458>
- Morita, Y., Ohshima, T., Nashiyama, I., Yamamoto, Y., Kawasaki, O., Matsuda, S., 1997. Anomalous degradation in silicon solar cells subjected to high-fluence proton and electron irradiations. *J Appl Phys* 81, 6491–6493. <https://doi.org/10.1063/1.364437>
- Nikolić, D., Stanković, K., Timotijević, L., Rajović, Z., Vujisić, M., 2013. Comparative study of gamma radiation effects on solar cells, photodiodes, and phototransistors. *International Journal of Photoenergy* 2013, 843174. <https://doi.org/10.1155/2013/843174>
- Nikolić, D., Vasić-Milovanović, A., Obrenović, M., Dolićanin, E., 2015. Effects of successive gamma and neutron irradiation on solar cells. *Journal of Optoelectronics and Advanced Materials* 17, 351–356.
- Pellegrino, C., Gagliardi, A., Zimmermann, C.G., 2019. Difference in space-charge recombination of proton and electron irradiated GaAs solar cells. *Progress in Photovoltaics: Research and Applications* 27, 379–390. <https://doi.org/10.1002/pip.3100>
- Raider, S.I., Flitsch, R., Aboaf, J.A., Pliskin, W.A., n.d. Surface Oxidation of Silicon Nitride Films.
- Robertson, J., 1993. Electronic Structure of Defects in Amorphous Silicon Nitride. *MRS Online Proceedings Library* 284, 65–76. <https://doi.org/https://doi.org/10.1557/PROC-284-65>
- Sato, S. ichiro, Miyamoto, H., Imaizumi, M., Shimazaki, K., Morioka, C., Kawano, K., Ohshima, T., 2009. Degradation modeling of InGaP/GaAs/Ge triple-junction solar cells

irradiated with various-energy protons. *Solar Energy Materials and Solar Cells* 93, 768–773. <https://doi.org/10.1016/j.solmat.2008.09.044>

Schmidt, J., Aberle, A.G., 1999. Carrier recombination at silicon-silicon nitride interfaces fabricated by plasma-enhanced chemical vapor deposition. *J Appl Phys* 85, 3626–3633. <https://doi.org/10.1063/1.369725>

Schnabel, M., Schulte-Huxel, H., Rienäcker, M., Warren, E.L., Ndione, P.F., Nemeth, B., Klein, T.R., Van Hest, M.F.A.M., Geisz, J.F., Peibst, R., Stradins, P., Tamboli, A.C., 2020. Three-terminal III-V/Si tandem solar cells enabled by a transparent conductive adhesive. *Sustain Energy Fuels* 4, 549–558. <https://doi.org/10.1039/c9se00893d>

Schygulla, P., Müller, R., Lackner, D., Höhn, O., Hauser, H., Bläsi, B., Predan, F., Benick, J., Hermle, M., Glunz, S.W., Dimroth, F., 2022. Two-terminal III-V//Si triple-junction solar cell with power conversion efficiency of 35.9 % at AM1.5g. *Progress in Photovoltaics: Research and Applications* 30, 869–879. <https://doi.org/10.1002/pip.3503>

Sharma, D., Mehra, R., Raj, B., 2022. Methods for Integration of III-V Compound and Silicon Multijunction for High Efficiency Solar Cell Design. *Silicon* 14, 9797–9804. <https://doi.org/10.1007/s12633-022-01691-x>

Sharma, V., Tracy, C., Schroder, D., Flores, M., Dauksher, B., Bowden, S., 2013. Study and manipulation of charges present in silicon nitride films, in: Conference Record of the IEEE Photovoltaic Specialists Conference. Institute of Electrical and Electronics Engineers Inc., pp. 1288–1293. <https://doi.org/10.1109/PVSC.2013.6744377>

Shen, X.B., Aierken, A., Heini, M., Mo, J.H., Lei, Q.Q., Zhao, X.F., Sailai, M., Xu, Y., Tan, M., Wu, Y.Y., Lu, S.L., Li, Y.D., Guo, Q., 2019. Degradation analysis of 1 MeV electron and 3 MeV proton irradiated InGaAs single junction solar cell. *AIP Adv* 9, 075205. <https://doi.org/10.1063/1.5094472>

Srour, J.R., Marshall, C.J., Marshall, P.W., 2003. Review of displacement damage effects in silicon devices. *IEEE Trans Nucl Sci* 50, 653–670. <https://doi.org/10.1109/TNS.2003.813197>

Summers, G.P., Burke, E.A., Xapsos, M.A., 1995. Displacement damage analogs to ionizing radiation effects. *Radiat Meas* 24, 1–8. [https://doi.org/10.1016/1350-4487\(94\)00093-G](https://doi.org/10.1016/1350-4487(94)00093-G)

Taylor, S.J., Yamaguchi, M., Yang, M.J., Imaizumi, M., Matsuda, S., Kawasaki, O., Hisamatsu, T., 1997. Type conversion in irradiated silicon diodes. *Appl Phys Lett* 70, 2165–2167. <https://doi.org/10.1063/1.118946>

Tobnaghi, D.M., Rahnamaei, A., Vajdi, M., 2014. Experimental Study of Gamma Radiation Effects on the Electrical Characteristics of Silicon Solar Cells. *Int. J. Electrochem. Sci.* 9, 2824–2831.

Verduci, R., Romano, V., Brunetti, G., Yaghoobi Nia, N., Di Carlo, A., D'Angelo, G., Ciminelli, C., 2022. Solar Energy in Space Applications: Review and Technology Perspectives. *Adv Energy Mater.* <https://doi.org/10.1002/aenm.202200125>

Weiss, C., Park, S., Lefèvre, J., Boizot, B., Mohr, C., Cavani, O., Picard, S., Kurstjens, R., Niewelt, T., Janz, S., 2020. Electron and proton irradiation effect on the minority carrier

1 lifetime in SiC passivated p-doped Ge wafers for space photovoltaics. Solar Energy
2 Materials and Solar Cells 209, 110430. <https://doi.org/10.1016/j.solmat.2020.110430>

3 Yamaguchi, M., 2001. Radiation-resistant solar cells for space use. Solar Energy Materials
4 and Solar Cells 68, 31–53. [https://doi.org/10.1016/S0927-0248\(00\)00344-5](https://doi.org/10.1016/S0927-0248(00)00344-5)

5 Yan, G., Wang, J. ling, Liu, J., Liu, Y. yu, Wu, R., Wang, R., 2020. Electroluminescence
6 analysis of VOC degradation of individual subcell in GaInP/GaAs/Ge space solar cells
7 irradiated by 1.0 MeV electrons. J Lumin 219, 116905.
8 <https://doi.org/10.1016/j.jlumin.2019.116905>

9 Yang, J., Bao, Q., Shen, L., Ding, L., 2020. Potential applications for perovskite solar cells in
10 space. Nano Energy. <https://doi.org/10.1016/j.nanoen.2020.105019>

11 Yang, S.-S., Gao, X., Wang, Y.-F., Feng, Z.-Z., 2011. Displacement Damage Characterization
12 of Electron Radiation in Triple-Junction GaAs Solar Cells. J Spacecr Rockets 48, 23–26.
13 <https://doi.org/10.2514/1.48873>

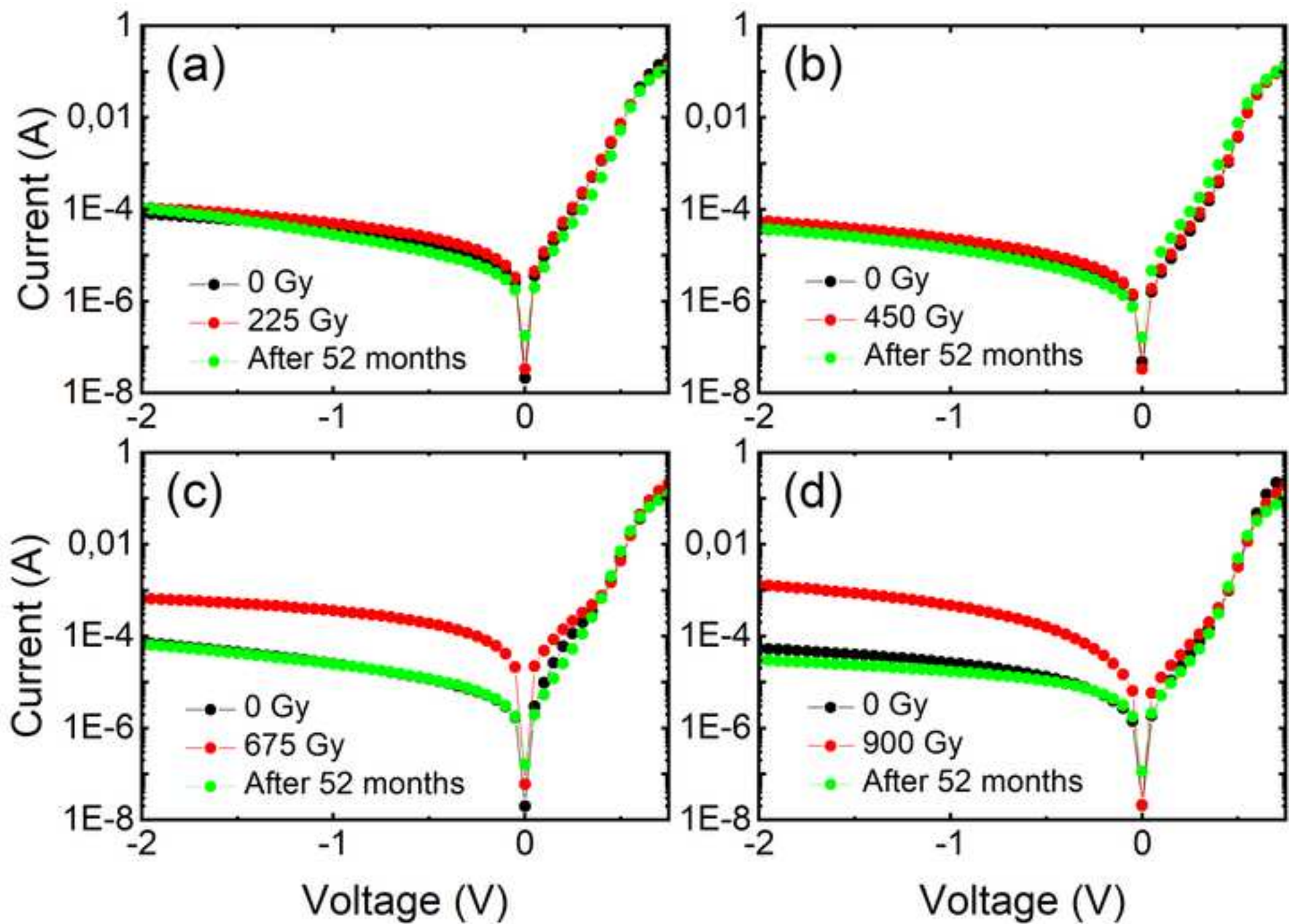
14 Yu, S., Rabelo, M., Yi, J., 2022. A Brief Review on III-V/Si Tandem Solar Cells.
15 Transactions on Electrical and Electronic Materials. <https://doi.org/10.1007/s42341-022-00398-5>

16 Zdravković, M.R., Vasić, A.I., Radosavljević, R.L., Vujišić, M.L., Osmokrović, P. V., 2011.
17 Influence of radiation on the properties of solar cells. Nuclear Technology and Radiation
18 Protection 26, 158–163. <https://doi.org/10.2298/NTRP1102158Z>

19 Zhang, Y., Qi, C., Wang, T., Ma, G., Tsai, H.S., Liu, C., Zhou, J., Wei, Y., Li, H., Xiao, L.,
20 Ma, Y., Wang, D., Tang, C., Li, J., Wu, Z., Huo, M., 2020. Electron Irradiation Effects
21 and Defects Analysis of the Inverted Metamorphic Four-Junction Solar Cells. IEEE J
22 Photovolt 10, 1712–1720. <https://doi.org/10.1109/JPHOTOV.2020.3025442>

23 Zhang, Y., Zhang, H., Yu, B., Wang, W., Hou, R., Chen, B., Xu, Q., Zhou, Y., Qin, G., 2014.
24 Gamma-ray irradiation hardness of arrayed silicon microhole-based radial p-n junction
25 solar cells. J Phys D Appl Phys 47, 065101. <https://doi.org/10.1088/0022-3727/47/6/065101>

1
2
3
4
5
6
7
8
9
10
11
12
13
14
15
16
17
18
19
20
21
22
23
24
25
26
27
28
29
30
31
32
33
34
35
36
37
38
39
40
41
42
43
44
45
46
47
48
49
50
51
52
53
54
55
56
57
58
59
60
61
62
63
64
65



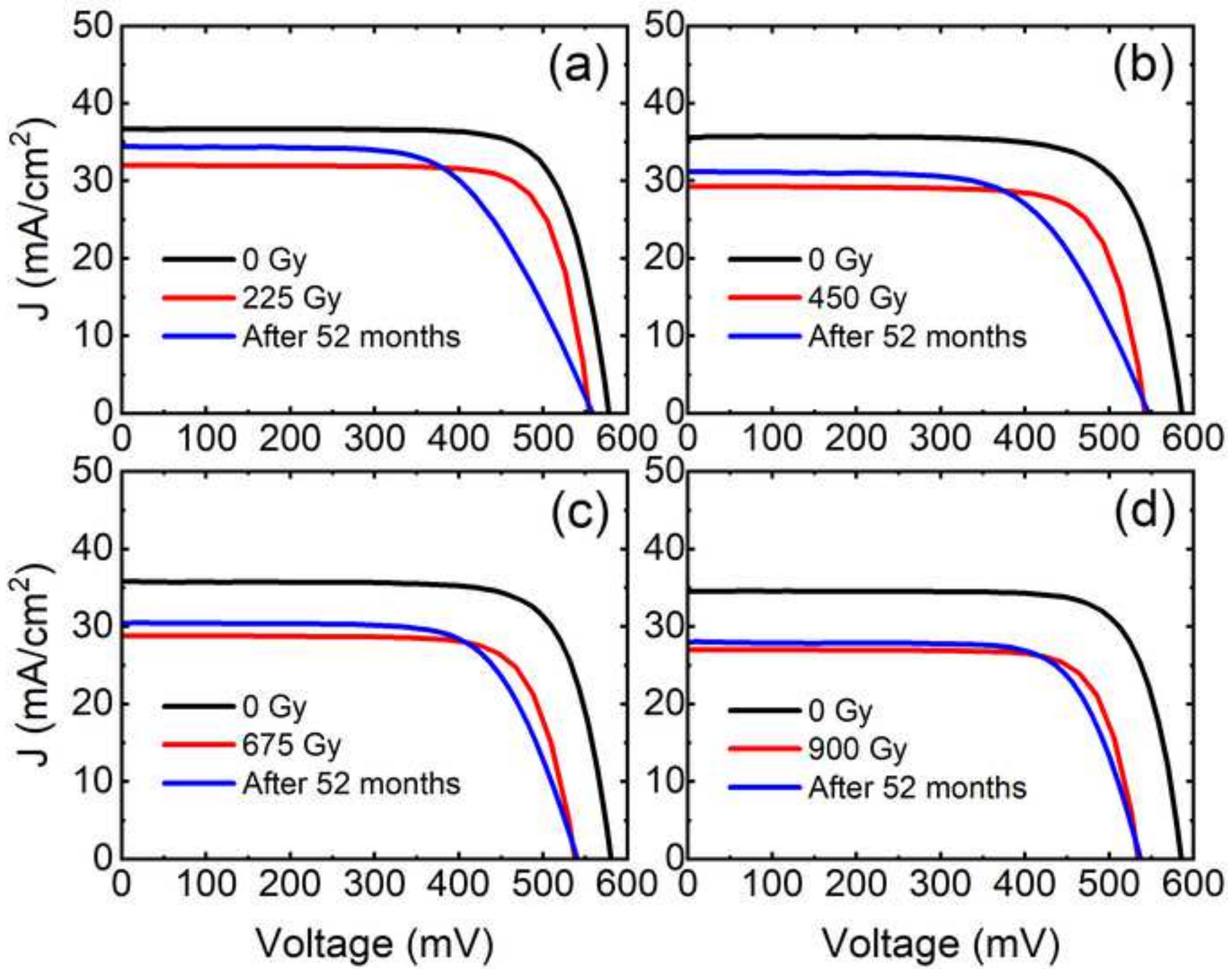


Figure 3a

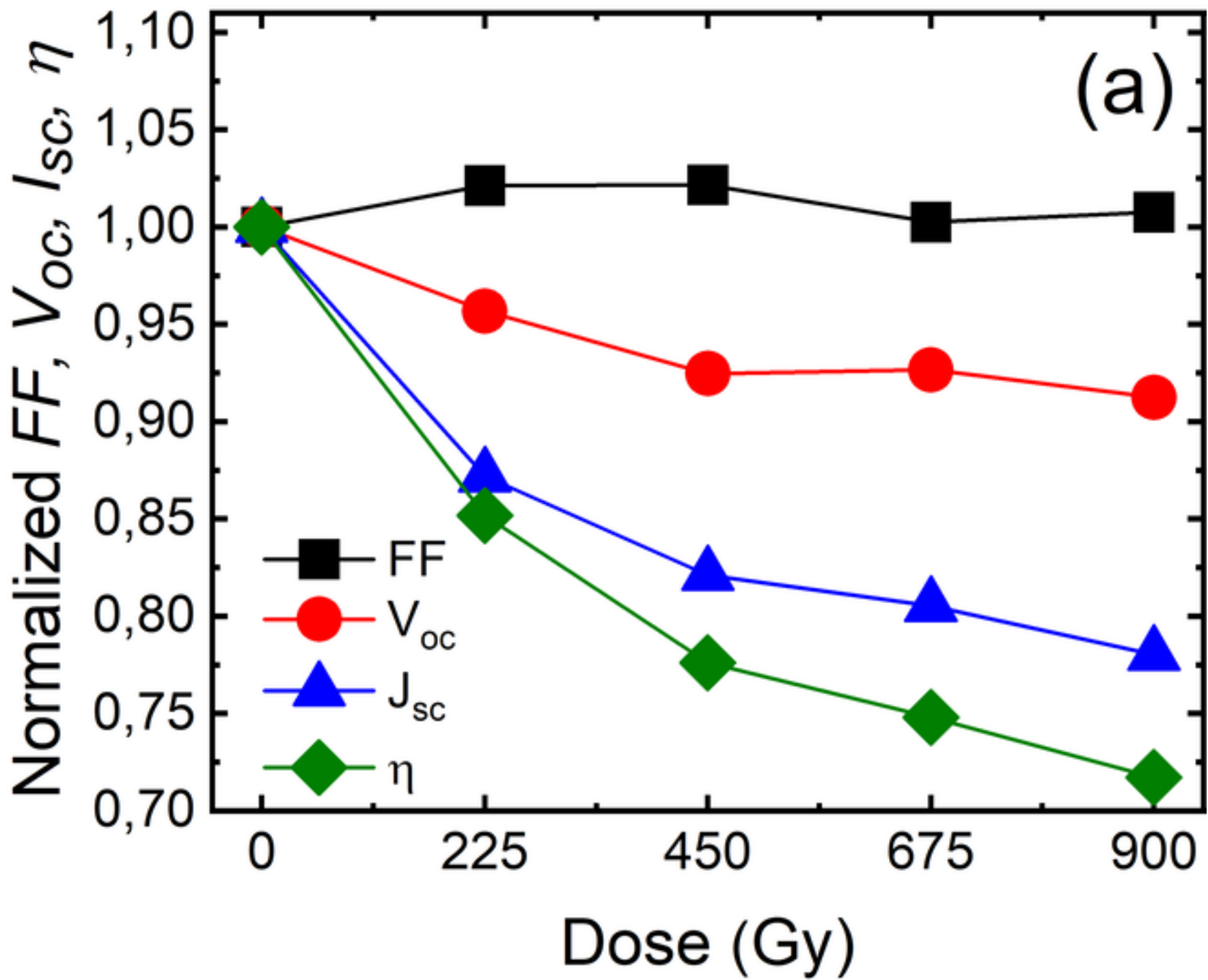
[Click here to access/download;Figure;Figure 3a.jpg](#)

Figure 3b

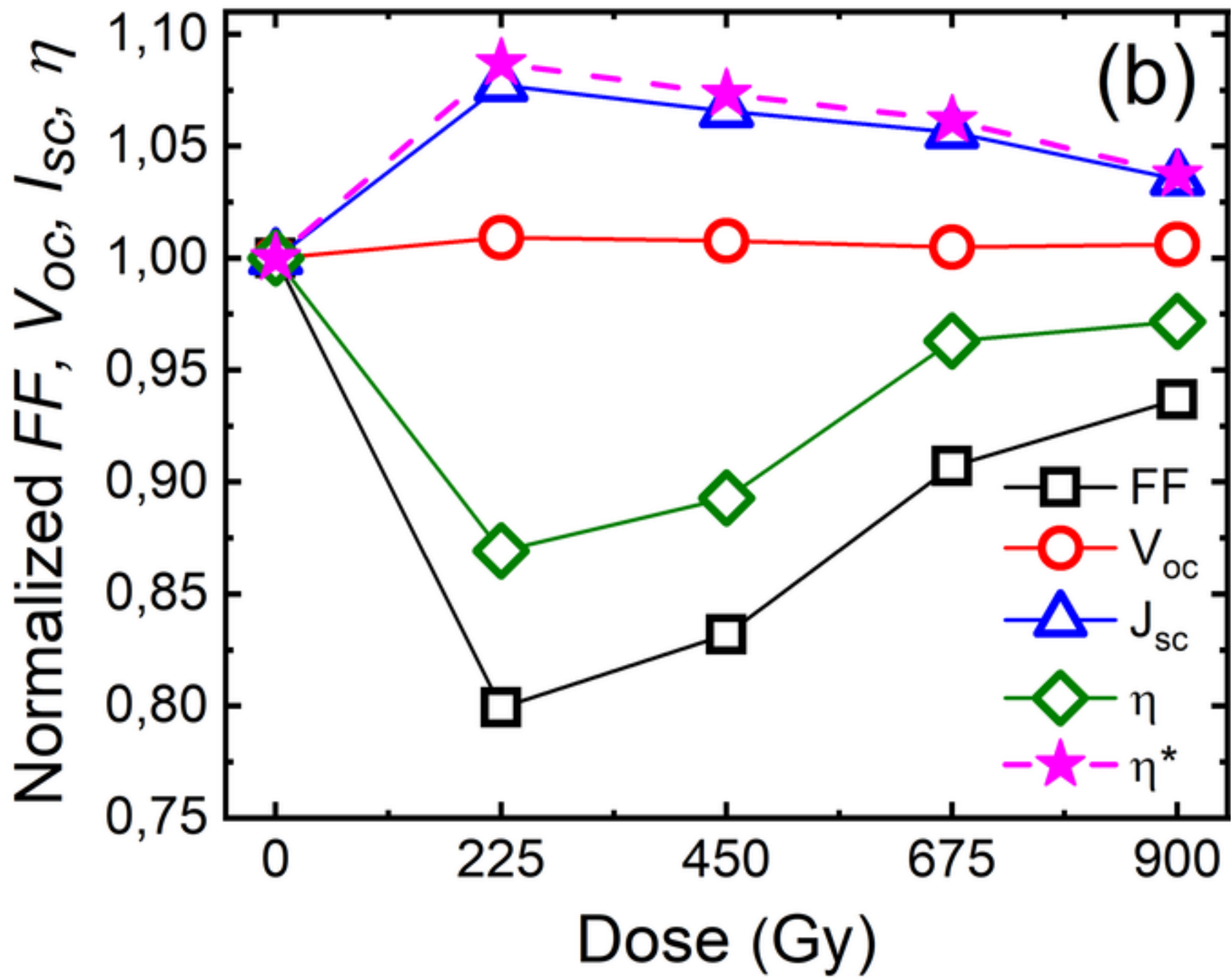
[Click here to access/download;Figure;Figure 3b.jpg](#)

Figure 4

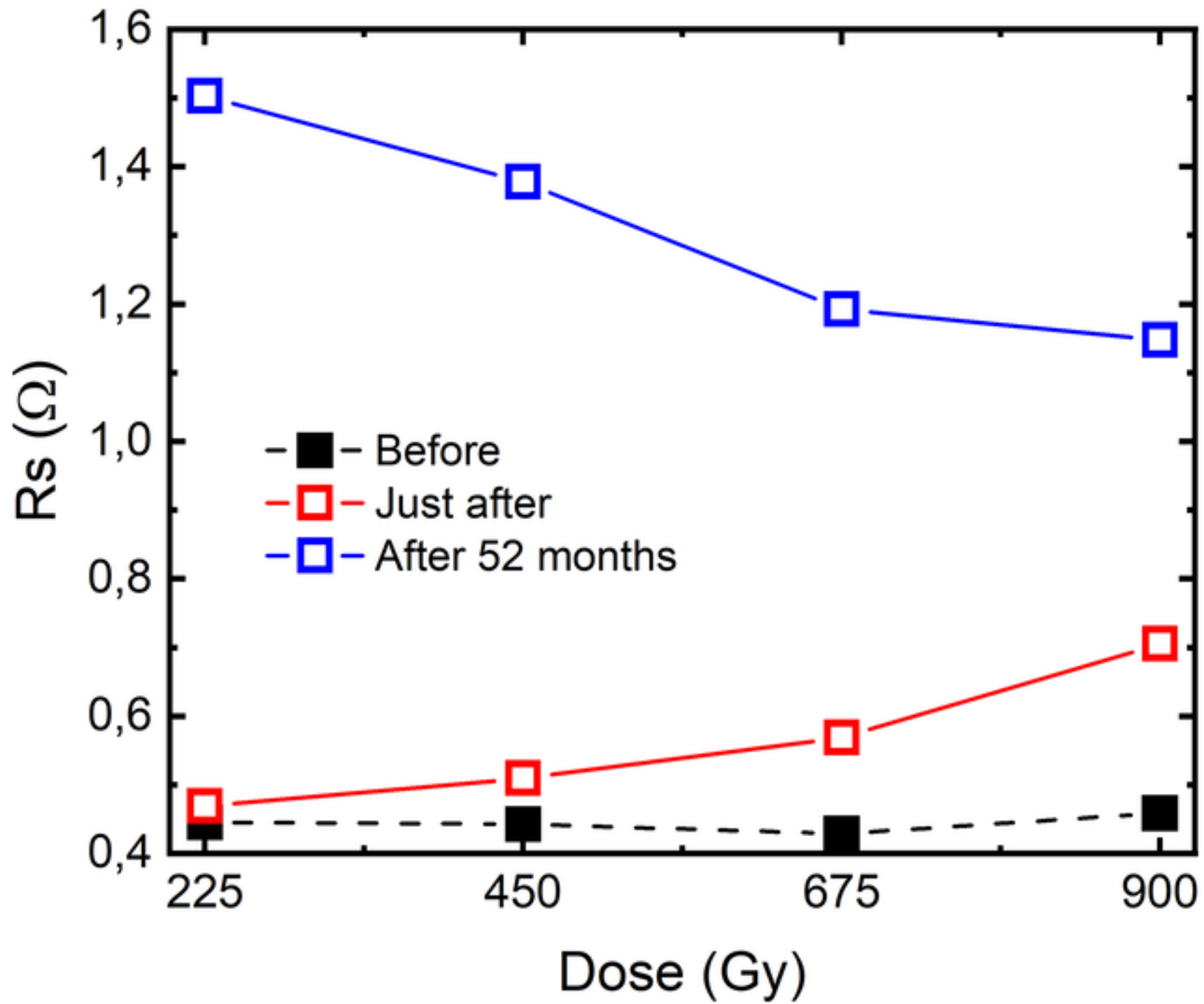
[Click here to access/download;Figure;Figure 4.jpg](#)

Figure 5

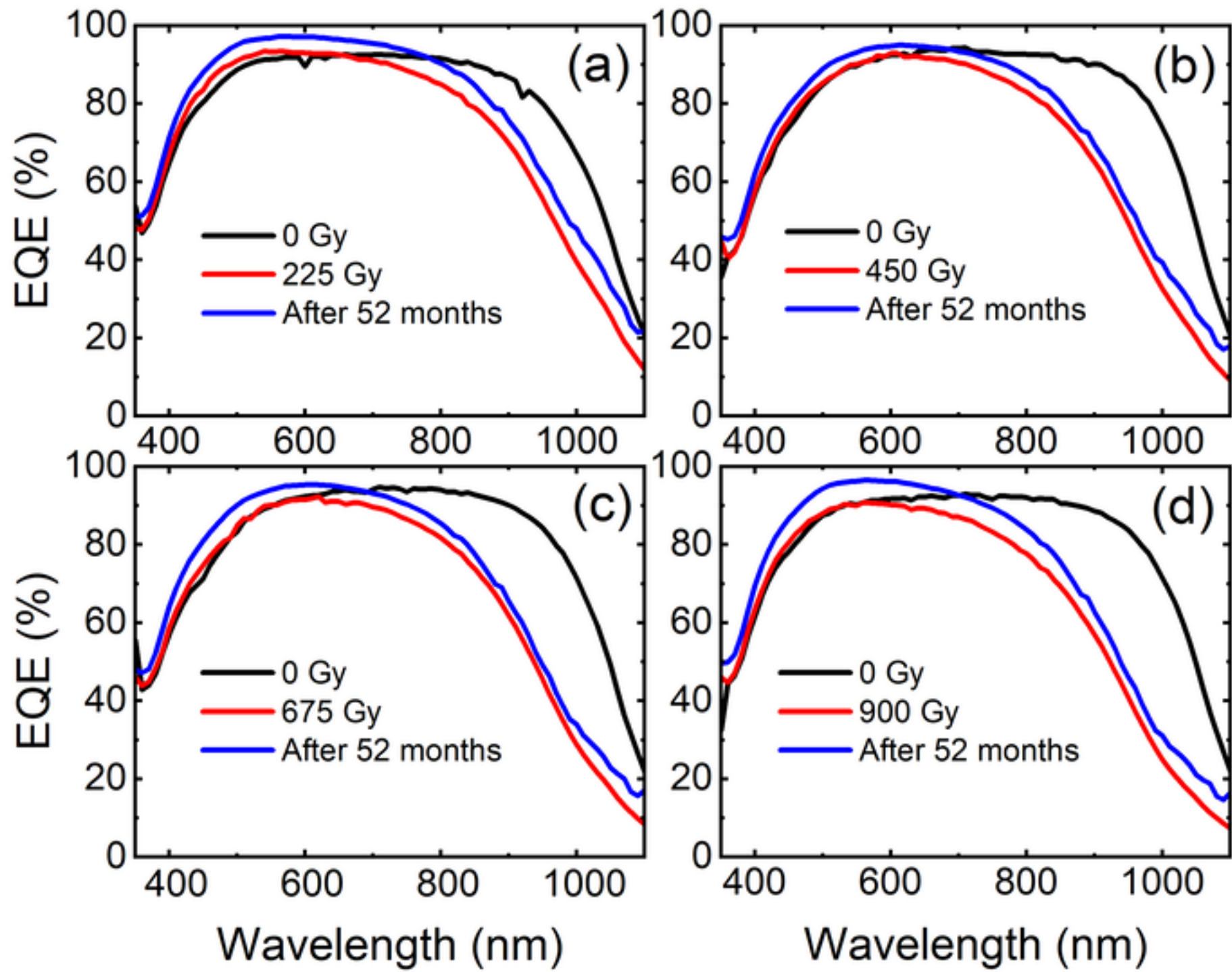
[Click here to access/download;Figure;Figure 5.jpg](#)

Figure 6

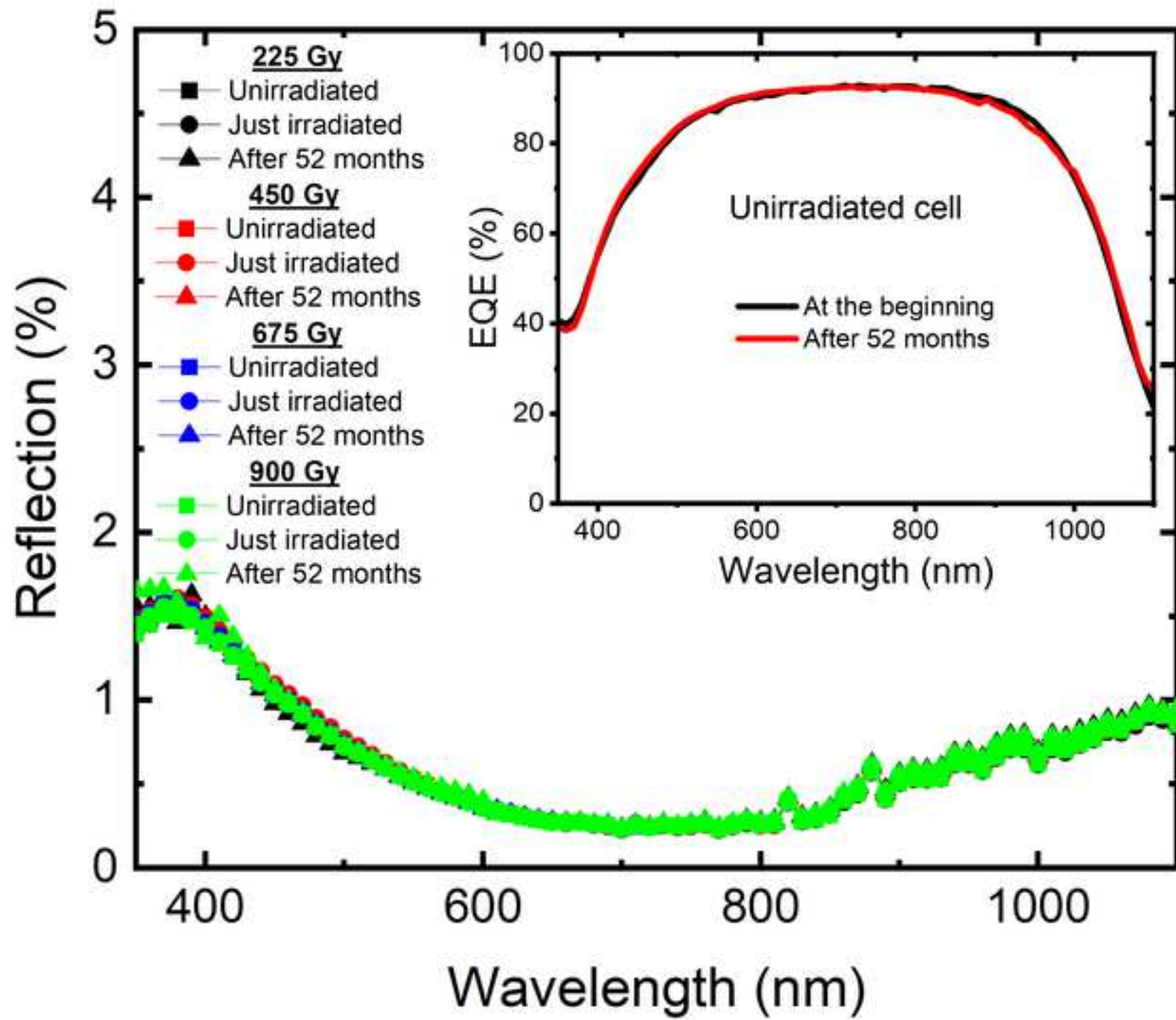
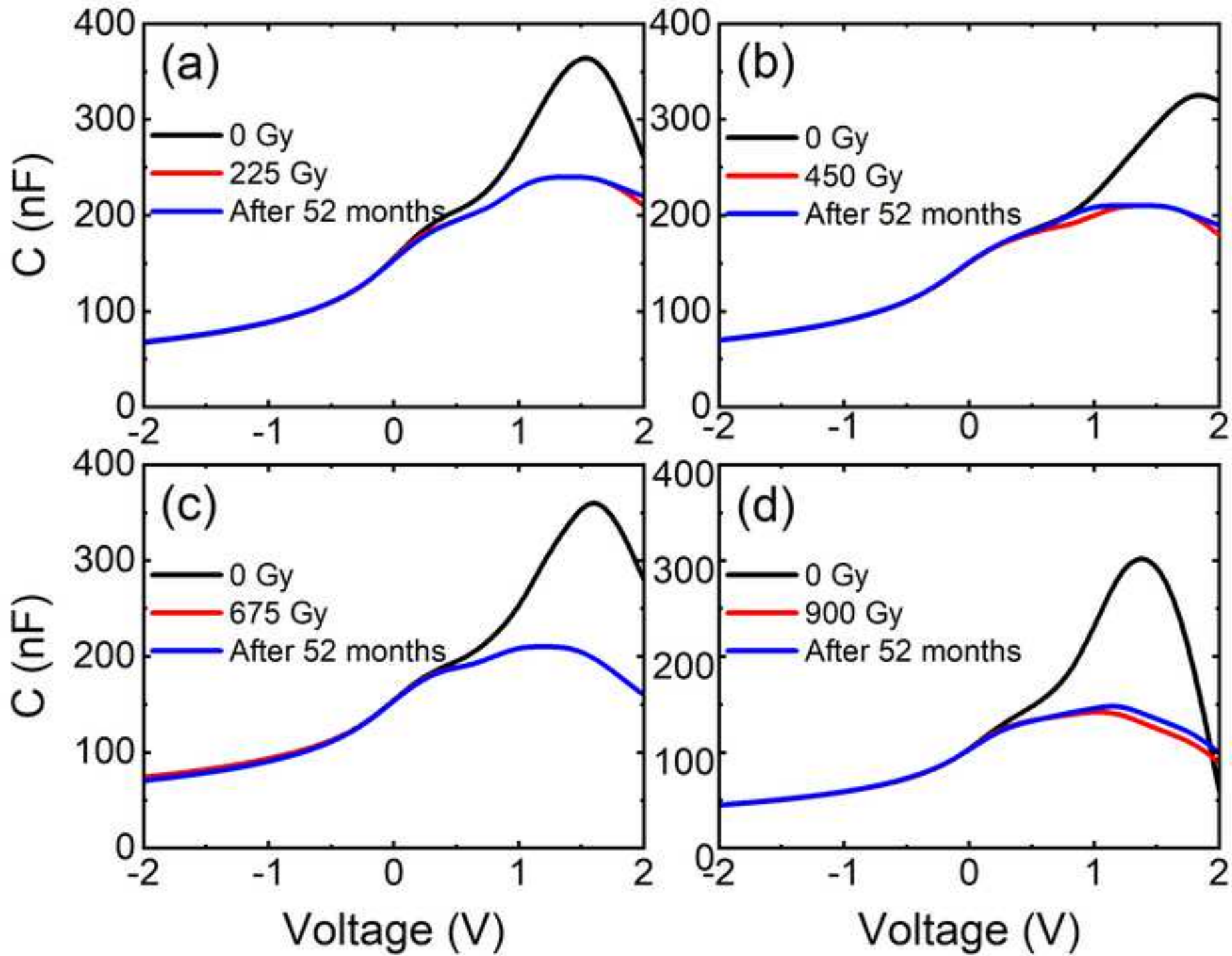
[Click here to access/download;Figure;Figure 6.jpg](#)

Figure 7

[Click here to access/download;Figure;Figure 7.jpg](#)

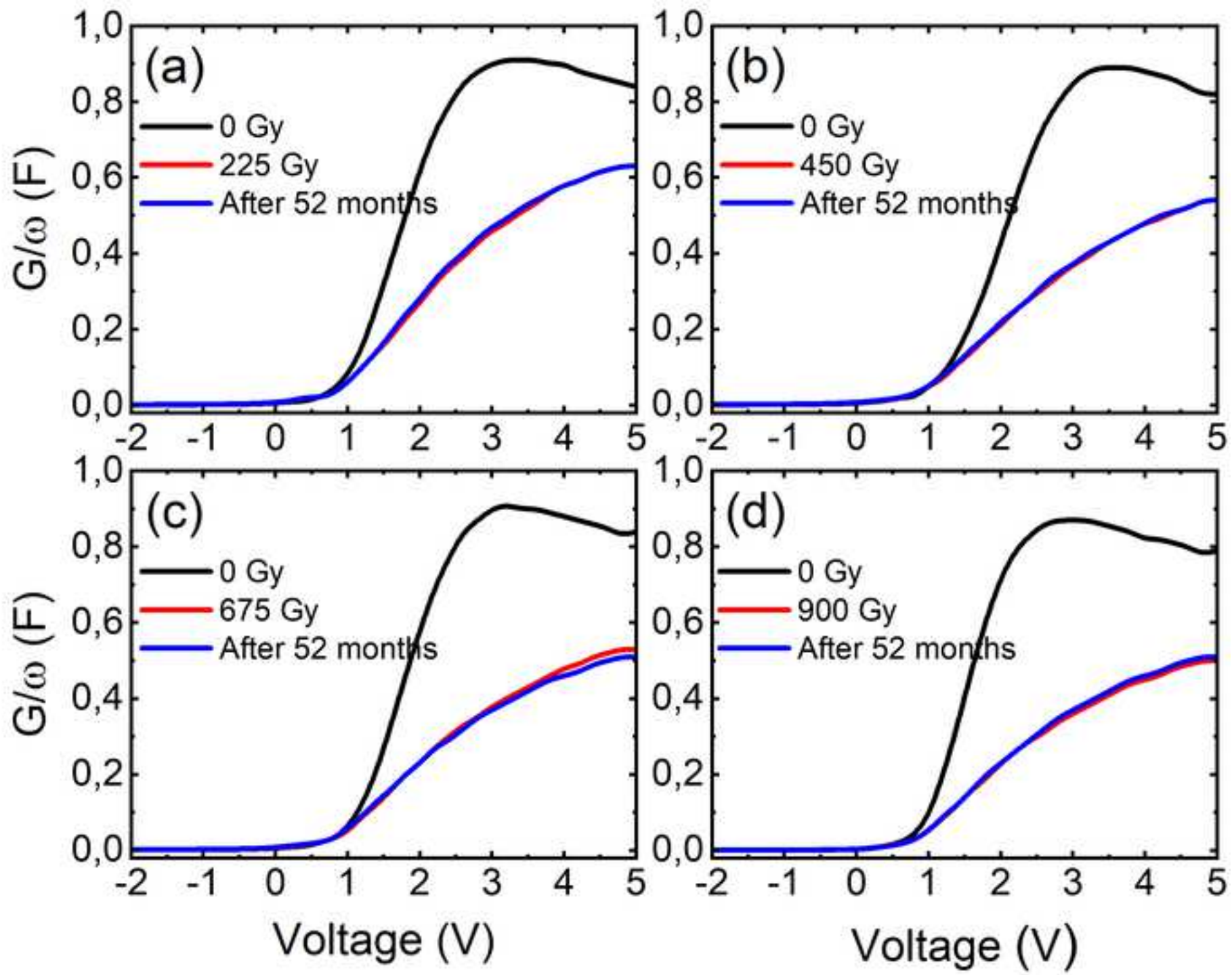


Table 1. Calculated diode ideality factors of the cells.

	225 Gy	450 Gy	675 Gy	900 Gy
Unirradiated	1.71	1.67	1.62	1.76
Just after Irradiation	1.86	1.94	2.18	2.43
After 52 months of irradiation	1.74	2.08	1.95	2.13

Table 2. Calculated loss and recovery in J_{SC} values from illuminated I-V measurements (Fig. 2) for different radiation doses. J_{SC0} , J_{SC1} and J_{SC2} are the short circuit current densities of the cells before irradiation, just after irradiation and after a 52-month period of irradiation respectively.

Dose (Gy)	Loss in J_{SC} ($J_{SC0} - J_{SC1}$) (mA/cm ²)	Recovery in J_{SC} ($J_{SC2} - J_{SC1}$) (mA/cm ²)	Percentage in J_{SC} recovery (%)
225	4.70	2.47	52.6
450	6.37	1.92	30.1
675	6.97	1.62	23.2
900	7.60	1.23	16.2

Table 3. Calculated loss and recovery in JSC values from EQE measurements (Fig. 5) for different radiation doses. JSC0, JSC1 and JSC2 are the short circuit current densities of the cells for unirradiated, just irradiated and after 52 months of irradiation cases respectively.

Dose (Gy)	Loss in JSC ($J_{SC0} - J_{SC1}$) (mA/cm ²)	Recovery in JSC ($J_{SC2} - J_{SC1}$) (mA/cm ²)	Percentage in JSC recovery (%)
225	2.75	2.24	81.5
450	4.62	1.73	37.4
675	5.36	1.89	35.3
900	5.87	2.60	44.3